

The genetic control of plant mitochondrial morphology and dynamics

David C. Logan*, Iain Scott and Alyson K. Tobin

School of Biology, Sir Harold Mitchell Building, University of St Andrews, St Andrews, Fife KY16 9TH, Scotland, UK

Received 18 June 2003; revised 6 August 2003; accepted 13 August 2003.

*For correspondence (fax +44 1334 463366; e-mail david.logan@st-and.ac.uk).

Summary

Little is known about the genetic control of mitochondrial morphology and dynamics in higher plants. We used a genetic screen involving fluorescence microscopic analysis of ethyl methane sulphonate (EMS)-mutated *Arabidopsis thaliana* seedlings expressing GFP targeted to mitochondria to isolate eight mutants displaying distinct perturbations of the normal mitochondrial morphology or distribution. We describe five mutants with distinct and unique mitochondrial phenotypes, which map to five different loci, not previously implicated in mitochondrial behaviour in plants. We have used a combination of forward and reverse genetics to identify one of the genes, *friendly mitochondria (FMT)*, a homologue of the *CluA* gene of *Dictyostelium discoideum*, which is involved in the correct distribution of mitochondria in the cell. The five mutants constitute a powerful resource to aid our understanding of mitochondrial dynamics in higher plants.

Keywords: mitochondria, plastids, organelle dynamics, membrane morphology, *Arabidopsis*.

Introduction

Mitochondria are ubiquitous and vital eukaryotic organelles. Although identified over 50 years ago as the sites of oxidative energy metabolism (Kennedy and Lehninger, 1949), it is only in the past decade that researchers, predominantly working with yeast, have elucidated the basic mechanisms controlling mitochondrial shape, size and number in this organism (for review, see Catlett and Weisman, 2000; Shaw and Nunnari, 2002; Yaffe, 1999). These yeast-based studies not only provide an indication of the types of proteins that are likely to be involved in mitochondrial development in higher plants but also highlight two important facts. First, yeast mitochondrial morphology is fundamentally different from that in higher plants. In yeast cells, the 5–10 mitochondria are elongated, tubule-shaped organelles and form extensive mitochondrial networks in the cortical cytoplasm (Stevens, 1977), whilst in higher plants, the mitochondria (several hundreds in a typical epidermal cell) generally alternate between spherical and sausage-shaped structures (Logan and Leaver, 2000; Stickens and Verbelen, 1996). These morphological and organisational differences suggest differences in the control pathways for mitochondrial development between the two organisms. Second, searching the DNA and protein databases has failed to find plant homologues of many yeast proteins involved in mitochondrial develop-

ment such as: Fzo1p (Hales and Fuller, 1997); Mdv1p/Fis2/Gag3/Net2p (Cervený *et al.*, 2001; Fekkes *et al.*, 2000; Mozdy *et al.*, 2000; Tieu and Nunnari, 2000); Mmm1p (Burgess *et al.*, 1994); Mdm12p (Berger *et al.*, 1997); Mdm14p (Shepard and Yaffe, 1997); and Mdm20p (Hermann *et al.*, 1997). In some cases, the absence of homologues of the yeast proteins from the *Arabidopsis* proteome may be explained by the fundamental differences between yeast and plant mitochondrial morphology and reproductive biology. For example, the yeast *Saccharomyces cerevisiae* proliferates by budding whereby the mother cell produces a daughter bud that grows and eventually becomes an independent cell. An essential part of this process is the transport of mitochondria and other organelles into the daughter bud. Mmm1p, Mdm10p, Mdm12p, Mdm14p and Mdm20p are all involved in the transmission of mitochondria to the daughter buds (Yaffe, 1999), and as cell proliferation in plants occurs by cell division, these proteins are not required.

Mitochondria in various eukaryotic cells undergo continuous cycles of fission and fusion and these processes control the number, size and distribution of these organelles (Bereiter-Hahn and Voth, 1994; Catlett and Weisman, 2000; Shaw and Nunnari, 2002; Yaffe, 1999). Yeast mitochondrial fission is regulated by a GTPase, called Dnm1p

(Ostuga *et al.*, 1998), that is structurally related to the evolutionarily conserved dynamin-related proteins required for membrane scission during exocytosis (Damke *et al.*, 1994, 1995; Herskovits *et al.*, 1993; Hinshaw and Schmid, 1995; van der Bliek *et al.*, 1993). Dynamin-related proteins have also been implicated in mitochondrial division in mammals (Drp1, Smirnova *et al.*, 1998), nematodes (DRP-1, Labrousse *et al.*, 1999) and red algae (CmDnm1, Nishida *et al.*, 2003). A dynamin-related protein, ADL2b, has recently been shown to be involved in division of higher plant mitochondria (Arimura and Tsutsumi, 2002), but ADL2b is the only known component of the plant mitochondrial division apparatus. Nothing is known about the genes, proteins or mechanisms controlling mitochondrial fusion in higher plants.

As a precursor to identifying the genes, proteins and mechanisms controlling mitochondrial development in higher plants, we developed a mutant screening procedure based on the chemical mutagenesis of *Arabidopsis thaliana* plants expressing mitochondrial-targeted GFP. Using epifluorescent microscopy, we have identified eight mutants with distinct aberrant mitochondrial phenotypes. In the

present report, we present five novel plant mitochondrial development mutants and describe a combination of forward and reverse genetics studies that identify the gene responsible for one of these mutants, the friendly mitochondrial (*fmt*) mutant. This new gene, *FMT*, is required for correct mitochondrial distribution and morphology.

Results

Identification of novel plant mitochondrial development mutants

Eight novel mitochondrial mutants were identified from a population of 9500 M₂ seedlings, seven of which set seed and had heritable phenotypes and one mutant was sterile. Six of these mutants displayed phenotypes indicative of perturbations in mitochondrial development.

The five mutants presented here display striking mitochondrial phenotypes (Figure 1). In the first motley mitochondrial (*mnt1*) mutant, the mitochondrial population is highly heterogeneous varying in size from one

Figure 1. Epifluorescent (left-hand panels) and TEM micrographs (right-hand panels) of wild-type (wt) and mutant *Arabidopsis* leaf mitochondria.

Epifluorescent micrographs are false-coloured for GFP (green) and chlorophyll (red).

(a, b) Wild-type, arrows, mitochondria; *, chloroplast.

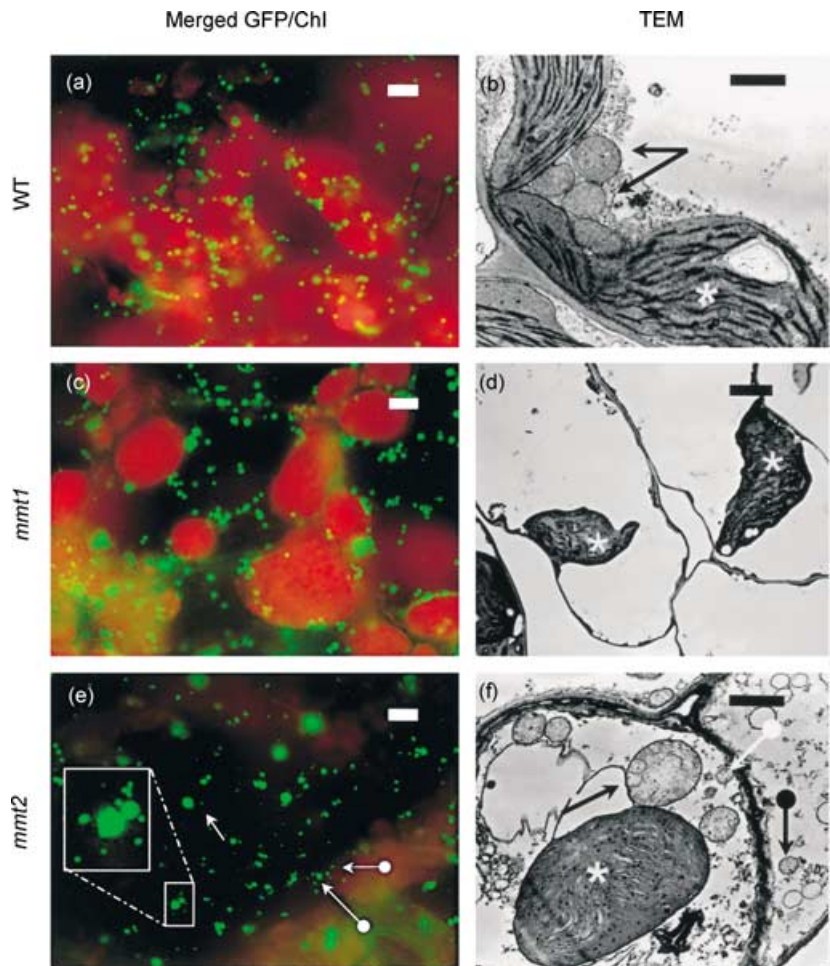
(c, d) *mnt1* mutant, *, chloroplast.

(e, f) *mnt2* mutant; plain arrows, large mitochondria; arrows with circle, small mitochondria; the boxes indicate an area magnified to highlight the heterogeneity of mitochondria size within a single cell; *, chloroplast with dense mass of internal membranes.

(g, h) *bmt* mutant; arrow, mitochondria.

(i, j) *nmt* mutant; arrows, small mitochondria; *, chloroplast.

(k, l) *fmt* mutant; arrow, large mitochondrial cluster; the boxes indicate an area magnified to highlight a large cluster of mitochondria; *, chloroplast. Scale bars in epifluorescent images = 5 μ m; in TEMs = 1 μ m, except in (f) where the bar = 5 μ m.



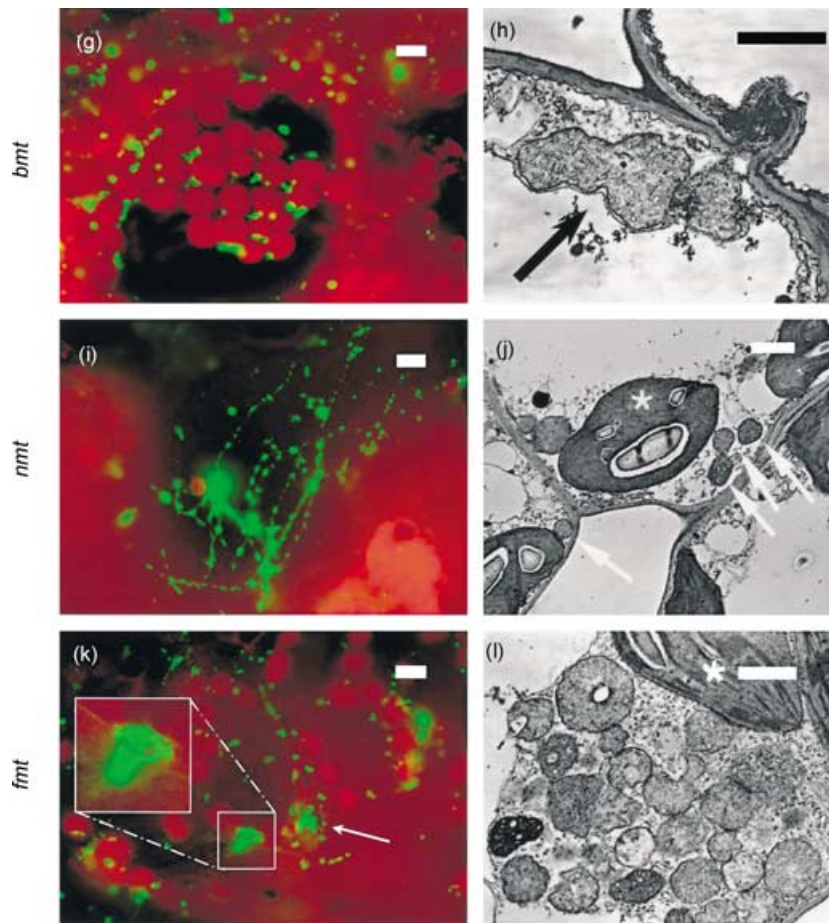


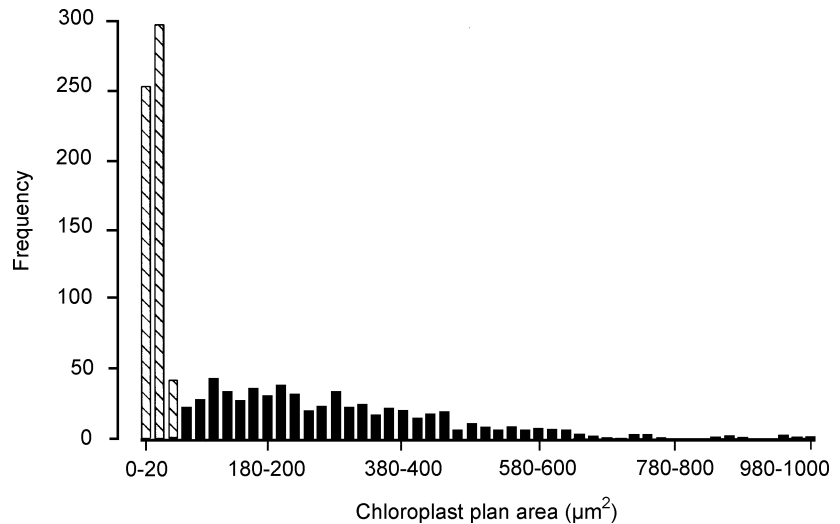
Figure 1. continued

quarter to four times as much as the average plan area of wild-type mitochondria (Figure 1c). In addition, chloroplast size is affected with the average plan area of chloroplasts in the mutant being $288.9 \pm 7.7 \mu\text{m}^2$ relative to $24.1 \pm 0.4 \mu\text{m}^2$ in the wild type. The size distribution of chloroplasts is also affected in the mutant. The plan area of wild-type chloroplasts range from 4.2 to $62.3 \mu\text{m}^2$ compared with 16.8 to $999.4 \mu\text{m}^2$ in the *mmt1* mutant (Figure 2). The second mutant *mmt2* contains a highly heterogeneous mitochondrial population similar to *mmt1*, although in this second mutant, the gross chloroplast morphology remains normal. Transmission electron microscopy (TEM) of the *mmt2* mutant, in addition to confirming the mitochondrial heterogeneity, demonstrated that the internal structure of the chloroplasts is severely altered (Figure 1f). Chloroplasts in the *mmt2* mutant contain a mass of densely packed membranes instead of the normal morphology of granal stacks connected by stromal lamellae, and there are a large number of electron dense particles within the chloroplasts.

The average plan area of mitochondria in the big mito-chondrial (*bmt*) mutant is two times as much as that of the wild type ($bmt = 0.98 \pm 0.04 \mu\text{m}^2$, $n = 660$; wild type

(wt) = $0.55 \pm 0.01 \mu\text{m}^2$, $n = 10009$), and there are approximately half as many mitochondria per microscope field-of-view (Figure 1g,h); there was no visible effect on chloroplast morphology in this mutant. The network mito-chondrial (*nmt*) mutant is characterised by the presence of long interconnected mitochondrial tubules (Figure 1i) extending to many tens of micrometers in length. Examination of leaf tissue of *nmt* plants under the TEM showed that the aberrant mitochondrial architecture was not maintained in the fixed tissue (Figure 1j), rather the mitochondrial tubules fragmented to form organelles as small as 1/16th the plan area of those in wild-type cells. As with *bmt*, chloroplast morphology in *nmt* was normal. Finally, the *fmt* mutant was identified by the presence of discrete clusters of tens of mitochondria in all cell types examined (Figure 1k,l). Only a proportion of the total mitochondrial complement of the cell formed aggregates and many mitochondria maintained a wild-type distribution. Examination of leaf tissue of this mutant by TEM revealed clusters of tens of mitochondria profiles in all cells examined, a typical cluster in a mesophyll cell is shown in Figure 1(l), confirming the phenotype observed *in vivo*. Chloroplast morphology in *fmt* was normal. To determine whether these clusters

Figure 2. Heterogeneity of chloroplast size in *mnt1* relative to wild-type. Frequency distribution of the plan areas of 600 chloroplasts each from wild-type (line 43A9, hatched bars) or *mnt1* (solid bars) seedlings.



comprised discrete mitochondria or were formed because of incomplete membrane severance during division, we analysed tens of ultra-thin sections under the TEM. The micrographs clearly show the clustered mitochondria as individual organelles, and we could find no evidence of membrane connections between adjacent mitochondria (Figure 3 and unpublished data).

Mapping the mutant loci

Genetic analysis of the progeny from backcrosses of *mnt2*, *bmt* and *fnt* to the wild type (line 43A9) revealed that these three phenotypes result from recessive mutations in single nuclear genes. Backcrossing *mnt1* gave a ratio of 1 : 6.5 (14 mutants: 91 wild type) in the F₂ because of a significantly ($P < 0.001$) lower average seed germination percentage

in the mutant (30.6%) relative to that of wild-type seed (89.6%). Repeated attempts to backcross *mnt* failed to produce seed.

To determine approximate chromosomal positions, we crossed each of the mutants, which are in Col-0 background, to wild-type Landsberg *erecta* (*Ler-0*) plants. F₂ mutants were identified by epifluorescence microscopy, and we used bulk segregant linkage analysis (Lukowitz *et al.*, 2000) to assign approximate chromosomal positions to the mutant loci. Map positions were refined using additional SSLP (Bell and Ecker, 1994), CAPS (Konieczny and Ausubel, 1993) and Cereon insertion or deletion (InDel) markers (Jander *et al.*, 2002). The *mnt1*, *mnt2*, *bmt* and *nmt* mutants were mapped to loci not previously implicated in mitochondrial or chloroplast development (Table 1). As a result of the similarity of the chloroplast phenotype of the *mnt1* mutant to several previously characterised accumulation and retention of chloroplast (*arc*) mutants (Marrison *et al.*, 1999; Pyke and Leech, 1992, 1994; Pyke *et al.*, 1994), we performed genetic complementation testing with *arc5*, *6*, *11* and *12*, which indicated that *mnt1* was not allelic to any of these genes (data not shown).

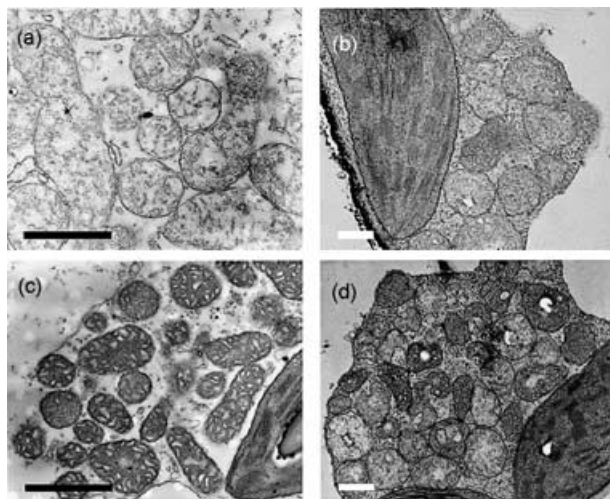


Figure 3. TEM micrographs of mitochondrial clusters in the *fnt* mutant. The four images (a–d) are representative of an analysis of over 40 clusters. Scale bar = 500 nm.

Table 1 Nearest linked markers flanking the mutant loci

Mutant	Chromosome	Flanking markers (north, south)
<i>mnt1</i>	II	ciw3 ^a , PHYB ^b
<i>mnt2</i>	IV	nga1139 ^a , nga1107 ^a
<i>bmt</i>	V	nga139 ^a , F18G18 ^c
<i>nmt</i>	V	F5024 ^d , MOP9 ^d
<i>fnt</i>	III	ciw4 ^a , AFC1 ^b

^aSSLP and ^bCAPS markers detailed on TAIR web site (<http://www.arabidopsis.org/>).

^cThe SSLP marker on BAC F18G18 and ^dInDel markers on BACS F5024 and MOP9 were PCR amplified using the primers given in the section under Experimental procedures.

FMT is the *Arabidopsis* homologue of the Dictyostelium discoideum *CluA* gene

We used a population of 41 F₂ mutants to map the *fmt* locus. Two markers were identified as flanking the mutant locus: *ciw4* (40 out of 41 mutants homozygous for the Col polymorphism) and *AFC1* (38 out of 41; Table 1). The three individuals heterozygous at *AFC1* were homozygous for the Col polymorphism using an InDel marker on BAC F4F15. These results demonstrated that the *fmt* locus is in a 3.9-cM stretch of chromosome III flanked by *ciw4* and *AFC1* and close to or within BAC F4F15.

The *fmt* phenotype is similar to the mitochondrial phenotype of the *cluA*-mutant of *D. discoideum* in which the mitochondria cluster near the cell centre (Zhu *et al.*, 1997). Inspection of the region containing the *fmt* locus revealed an *Arabidopsis* homologue of the *CluA* gene (*Atclu*) on BAC F4F15. When the *AtClu* gene was sequenced, a single point mutation was found at the first base of the second intron (+519 bases from the initial ATG). This G→A mutation destroys the first base of the intron–exon consensus motif GT...AG, which we predicted would prevent correct splicing. Consistent with this, *AtClu* transcript abundance, as detected by Northern blotting, was greatly reduced (Figure 4).

Reverse genetics confirms the role of the *Atclu* gene in mitochondrial distribution

Two lines of evidence now support the proposition that the *fmt* phenotype is caused by disruption of the *Atclu* gene. To confirm this proposition, we decided to switch to a reverse genetics approach. An independent allele at the *AtClu* locus was recovered from the SAIL T-DNA insertion lines (Sessions *et al.*, 2002) and transformed by infiltration with *Agrobacterium tumefaciens* containing the pBINmGFP5-*atpase* vector. GFP-positive T₁ transformants of the SAIL line SAIL_284_D06 were screened under the epifluorescent microscope, and we identified three individual lines that had a clustered mitochondrial phenotype. These three lines were found to be homozygous for the insertion in the *AtClu* gene (Figure 5), while plants homozygous for the insertion displayed a wild-type phenotype (data not shown).

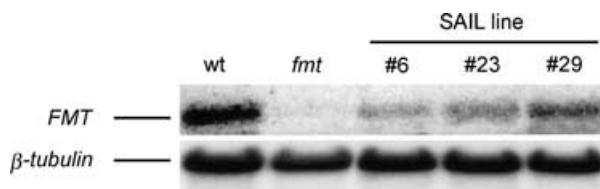


Figure 4. RNA gel blot analysis of the steady-state abundance of the *FMT* transcript in wild-type (wt) and mutant plants (*fmt* and three independent GFP-positive lines (6, 23 and 29) derived from SAIL line SAIL_284_D06.

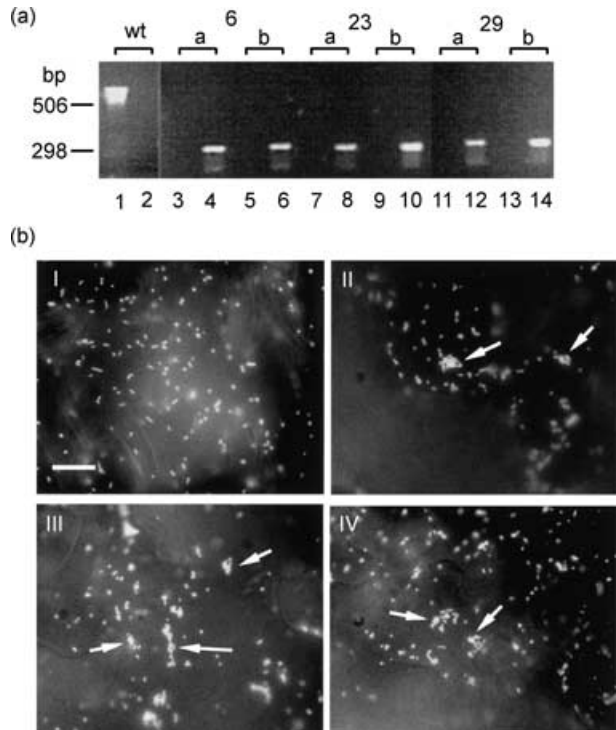


Figure 5. Analysis of SAIL lines containing a T-DNA insertion in the *FMT* gene.

(a) PCR analysis using gene-specific forward (Gf) and reverse (Gr) primers or the Gr primer and a primer to the T-DNA left border (LB3). Under the conditions used, PCR amplification using wild-type (wt) DNA yields a fragment only with the gene-specific primers, whilst amplification of a smaller DNA fragment using the Gr and LB3 primers indicates the presence of a T-DNA insertion. PCR amplification from DNA extracted from plants homozygous for the insertion would yield a product using both sets of primers, while PCR amplification of DNA from plants homozygous for the insertion would only yield a product using the LB3 and Gr primer set. DNA was extracted from wt (line 43A9) and in duplicate (a,b) from three independent GFP-positive lines (6, 23 and 29) derived from SAIL line SAIL_284_D06. Reactions from PCRs using the primer sets Gf/Gr (odd-numbered lanes) and Gr/LB3 (even-numbered lanes) were run in adjacent lanes. bp, positions of DNA molecular weight markers in base pairs.

(b) Epifluorescent micrographs of leaf epidermal cell mitochondria in mito-GFP transformed plants. I, wt (line 43A9); II–IV, independent GFP-positive lines 6, 23 and 29, respectively, of SAIL line SAIL_284_D06 (arrows indicate mitochondrial clusters). Scale bar = 10 μm.

We conclude that the *fmt* mutant phenotype results from a single point mutation in the *Arabidopsis* homologue of the *D. discoideum* *CluA* gene and therefore name the previously uncharacterised wild-type *Arabidopsis* gene *FMT*.

Discussion

In this paper, we describe the results of a novel genetic screen based on the analysis of ethyl methane sulphonate (EMS) mutants of an *Arabidopsis* line expressing mitochondrial-targeted GFP. This screen enabled the unprecedented identification and analysis of plant mitochondrial development mutants. Gene mapping of these mutants has

demonstrated that in each case, the mutant represents a locus not previously implicated in the control of plant mitochondrial morphology or distribution. Three mutants, *bmt*, *mmt1* and *mmt2* have novel phenotypes that have not, to our knowledge, been described in any organism. The *mmt1* phenotype is unique as far as both mitochondrial and chloroplast gross morphologies are affected. Although the mutant chloroplast morphology in *mmt1* is similar to that in several *arc* mutants (Marrison *et al.*, 1999; Pyke and Leech, 1992, 1994; Pyke *et al.*, 1994), complementation analysis has shown that *mmt1* is not allelic to *arc5*, *6*, *11* or *12*. No mention was made in the published studies of the *arc* mutants of any aberrant mitochondrial morphology, but it is possible that any changed morphology may only be visible in unfixed tissue. We are in the process of transforming *arc5*, *6*, *11* and *12* with the mitochondrial-GFP construct to enable *in vivo* visualisation of the mitochondrial morphology in these mutants. The *nmt* mutant displays a tubular/fused mitochondrial phenotype, which is similar to that observed in plant cells transiently expressing a dominant-negative mutation of the *Arabidopsis* dynamin-like protein ADL2b (Arimura and Tsutsumi, 2002). However, gene mapping has demonstrated that neither ADL2b nor any of the other 10 *Arabidopsis* dynamin-like genes are possible candidates for the *nmt* locus. Interrogation of the *Arabidopsis* genome databases reveals no obvious gene candidates within the mapping-delimited regions for any of these four mutants.

A combination of forward and reverse genetics revealed that the phenotype of a fifth mutant, *fmt*, was due to a single point mutation in a homologue of the *cluA* gene from *D. discoideum* to which we give the name *FMT*. Disruption of *cluA* in *Dictyostelium* causes the mitochondria to cluster near the cell centre (Zhu *et al.*, 1997). There are *cluA* homologues present as open-reading frames in all eukaryotic genomes sequenced to date, but, apart from a short tetrapeptide repeat (TPR) domain that is thought to function in protein-protein interactions, the CluA protein has no homology to known proteins. The *Arabidopsis* CluA protein homologue FMT (locus: CAB41334) is 26% identical and 41% similar to the *Dictyostelium* protein and also contains a TPR-like domain. The *S. cerevisiae* CluA homologue, Clu1p (20% identical, 34% similar to the *Arabidopsis* protein; 24% identical, 39% similar to CluA) has also been shown to be involved in the maintenance of normal mitochondrial morphology and distribution (Fields *et al.*, 1998). Disruption of the *CLU1* gene resulted in collapse of the mitochondrial tubules to one side of the yeast cell (Fields *et al.*, 1998). Alignment of the *Dictyostelium*, *Arabidopsis* and *Saccharomyces* proteins reveals the most conserved region to contain the TPR-like domain. However, following a report by Vornlocher *et al.* (1999) demonstrating that Clu1p (named p135 in that paper) sometimes co-purifies with subunits of the eukaryotic translation initiation factor eIF3, *CLU1* and

cluA have been re-annotated in the databases as encoding putative eIF3 subunits. As deletion of Clu1p had no effect on eIF3 activity (Vornlocher *et al.*, 1999) and Clu1p homologues do not co-purify with eIF3 subunits from human or plant cells (Browning *et al.*, 2001), the re-classification of Clu-type genes, ignoring the physiological data by Zhu *et al.* (1997) and Fields *et al.* (1998) seems erroneous.

In a recent study, Fields *et al.* (2003) addressed the question of how CluA is involved in maintaining the normal distribution of mitochondria in *Dictyostelium* cells. Using nocodazole or cytochalasin A to disrupt microtubules or actin filaments, respectively, the authors demonstrated that these cytoskeletal elements were not necessary to maintain mitochondria in their normal, dispersed state (Fields *et al.*, 2003). However, as noted by these authors, these findings do not rule out a role for microtubules and/or actin filaments in the positioning of the mitochondria prior to drug treatment. Based on the results of the drug treatments and the observation of interconnections between adjacent mitochondria within the clusters in mutant cells, Fields *et al.* (2003) concluded that *cluA*⁻ cells were blocked at the stage of outer membrane scission during organelle fission and that the clustered mitochondria formed an extensive interconnected reticulum. Examination of over 40 mitochondrial clusters provided no consistent evidence of a similar occurrence in the *fmt* mutant. At least in *Arabidopsis* cells, disruption of *FMT* affected the distribution of mitochondria but did not appear to result in the production of a mitochondrial reticulum. We note, however, that differences in sample preparation may account for the differences observed between mutant *Arabidopsis* and *Dictyostelium* mitochondria. Fields *et al.* (2003) examined serial sections of cells prepared for the electron microscope by means of cryofixation, whereas we used multiple independent sections of leaf that was prepared using chemical fixation.

In plant cells, transport of mitochondria has been shown to rely on actin filaments (Olyslaegers and Verbelen, 1998; Van Gestel *et al.*, 2002). However, microtubules have been shown to have a role in the positioning and/or tethering of mitochondria (Van Gestel *et al.*, 2002). It is not clear if mitochondrial transport in *Dictyostelium* is predominantly actin- or microtubule-based. Mitochondria have been shown to associate with the microtubule-specific motor protein, kinesin (Khodjakov *et al.*, 1998) that binds cargo at the TPR domains in the kinesin light chains (Stenoien and Brady, 1997; Verhey *et al.*, 2001). When mitochondria are moving on actin filaments, they are presumably prevented from binding to microtubules until this is required to immobilise the mitochondria or effect small-scale adjustments to their position. Based on the phenotype of the *fmt* mutant and the presence of a TPR domain in FMT, we hypothesise that when mitochondria are moving on actin filaments, FMT binds to the kinesin receptor on the mitochondria

via the TPR domains, thereby preventing any unwanted association with microtubules. This putative role of FMT as a cap for the kinesin receptor on the mitochondria leaves the microtubule-associated kinesin motor free to associate with other mitochondria or different types of cargo. Applying this hypothesis to the *fmt* mutant, in which receptor-capping would not occur, leaves the mitochondria free to bind to microtubules, which prevents their movement on actin. A cluster of mitochondria then develops as mitochondria divide but are unable to move apart. This hypothesis is consistent with the lack of a clustered mitochondrial phenotype in *Clu*-mutants of *Caenorhabditis elegans* (M. Clarke, personal communication) as in this organism large-scale mitochondrial movement is microtubule-based. Application of our receptor-capping hypothesis for FMT function to the *Dictyostelium cluA*⁻ mutant suggests an explanation for the interconnections between clustered mitochondria reported by Fields *et al.* (2003). Final separation of mitochondria following division may require movement on the cytoskeleton, and therefore when this is prevented, because of inexorable binding to microtubules, the mitochondria remain connected. The absence of a similar phenotype in *Arabidopsis* may simply reflect differences in the architecture of the cytoskeleton or the contribution of movement to the division process. Further study is necessary to discover the precise role of this conserved gene in mitochondrial dynamics.

Little is known about the genes, proteins and mechanisms controlling mitochondrial dynamics in higher plants. Although most work on mitochondrial morphology has been carried out on yeast, this is a poor model system for higher plants. Homology searches of the *Arabidopsis* genome fail to identify homologues of many yeast mitochondrial development genes suggesting that there are fundamental differences in the control of higher plant mitochondrial morphology and dynamics. This is reflected in the results of our genetic screen where four of the five mutants described in this paper result from the mutation of novel genes. Together these mutants constitute a powerful resource that will help delineate the principles and mechanisms controlling this fundamental aspect of plant development.

Experimental procedures

Plants

Seeds were surface sterilised and germinated on MS-agar plates (Murashige and Skoog (MS) 1962, medium, 8% (w/v) agar (Type M, Sigma Chemical Co., St Louis, USA), 2% (w/v) sucrose, 0.5% (w/v) Mes, pH 5.8). For maximum synchronous germination, plates were kept in the dark at 4°C for 3 days before transfer to a controlled environment growth room (16 h day, 8 h night, 25°C). After a further 2 weeks, plants were transplanted to compost (Levington

F2, Scotts, Marysville, USA) and grown in a greenhouse under supplementary lighting and constant temperature of 25°C. For germination tests, 50–100 seeds per replicate ($n = 4$) were sown on MS-agar plates, stratified for 3 days and germinated as above for 7 days. Germination percentages (ratios) were arcsine-transformed prior to statistical analysis using the *t*-test.

Mutant isolation

In a previous study, efficient targeting of GFP to *Arabidopsis* mitochondria was achieved by engineering a chimaeric construct in which the sequence encoding the first 87 amino acids of the *Nicotiana plumbaginifolia* β -ATPase was ligated upstream of the mGFP5 cDNA (Logan and Leaver, 2000). Seeds of an *Arabidopsis* line homozygous for the β -atpase-gfp chimaera (line 43A9, Logan and Leaver, 2000) were mutagenized by soaking 2 g of seed in 0.2% (v/v) EMS for 16 h. Seeds were then washed in water three times for 2 h and sown in compost. M₂ seed was collected from 20 batches of c. 50 M₁ plants and stored at 4°C. M₂ seeds were surface sterilised, stratified and germinated on MS-agar plates as described above supplemented with 50 $\mu\text{g ml}^{-1}$ kanamycin. After 1 week, seedlings were transferred to fresh plates (c. 40 per 9-cm plate) and grown for a further week in a vertical orientation so that the roots grew along the agar surface. This procedure was repeated each weekday for a different M₂ seed batch; after samples from all 20 batches had been plated-out, the process was repeated starting again with the first batch. Two-week-old seedlings were screened for aberrant mitochondrial phenotypes by removing the first true leaf and mounting it in water on a microscope slide under a cover slip; in this way nine plants could be screened per slide. Slides were examined under an Olympus BX-40 epifluorescent microscope (Olympus Optical Co. (UK) Ltd, Southall, UK) fitted with cubes for GFP (Olympus U-M41001, excitation: 455–495 nm; dichroic mirror: 505 nm; barrier filter: 510–555 nm) and for chlorophyll autofluorescence (Olympus U-M41004, excitation: 534–588 nm, dichroic mirror: 595 nm, barrier filter: 609–683 nm). Visualisation of mitochondria was performed at 1000 \times using an oil-immersion objective (100 \times Universal Plan Fluorite, numerical aperture = 1.3, Olympus).

Image analysis

Epifluorescent micrographs were acquired using a monochrome digital camera (F-View, Soft Imaging System GmbH, Munster, Germany) and analysed using the ANALYSIS software package (Soft Imaging System GmbH). False-coloured merged images were created using Confocal Assistant (Bio-Rad, Hemel Hempstead, UK), and all images were prepared for reproduction using ADOBE PHOTOSHOP elements (Adobe, San Jose, USA). Chloroplast plan area was measured using the ANALYSIS software; 20 chloroplasts chosen at random and in any cellular orientation were measured in three images taken of the mesophyll cell layer of one of the first true leaves of 10 individual 7-day-old wild-type (line 43A9) or *mmt1* seedlings ($n = 20 \times 3 \times 10 = 600$). To determine mitochondrial plan area, epifluorescent micrographs were taken of 5 (bmt) or 10 (wild-type) randomly selected areas of epidermis from one of the first true leaves of each of 5 (bmt) or 10 (wild-type) 14-day-old *Arabidopsis* seedlings.

Electron microscopy

Leaf material of 14-day-old *Arabidopsis* seedlings was fixed for 2 h in 2.5% (v/v) glutaraldehyde in 100 mM sodium phosphate buffer,

pH 7.2. The material was then post-fixed in 1% (v/v) osmium tetroxide and embedded in Araldite (TAAB Laboratories Equipment Ltd, Aldermaston, UK). Ultra-thin sections were cut and stained with uranyl acetate followed by lead citrate prior to observation.

Genetic analysis and gene mapping

Crosses to either 43A9 (Col-0 background, backcross) or *Ler-0* were performed by dissecting and emasculating unopened buds and then using the stigmas as recipients for pollen from three opened flowers. Segregation of the mutant mitochondrial phenotype in the F_2 generation was analysed with the χ^2 test for goodness of fit.

To determine an approximate chromosomal position, F_2 mutants from the mutant:*Ler-0* cross were identified by epifluorescence microscopy when 2 weeks old and were transferred to compost. When the plants had flowered, 5–10 buds were removed, snap-frozen in liquid N_2 and stored at -80°C . DNA was extracted using a CTAB procedure and bulk-segregant analysis was performed using the 21 simple sequence length polymorphism (SSLP, Bell and Ecker, 1994) markers as described by Lukowitz *et al.* (2000). Additional CAPS (Konieczny and Ausubel, 1993), or SSLP markers were either selected for testing by interrogation of the *Arabidopsis* Information Resource (TAIR), or we designed primer sets to putative SSLP regions and tested them empirically. The SSLP marker on BAC F18G18 was PCR amplified using the primers 5'-GTGGTGC GGTTCAAATAGTAC-3' and 5'-CTAGCTTTT TAGCCG-CATC-3'. We also designed primers flanking putative polymorphic InDel sites annotated in the Cereon polymorphism database (Jander *et al.*, 2002), and these primers were tested empirically. The two InDel markers referred to in Table 1 were PCR amplified using the following primers: F5O24, 5'-GTACCGA-ATTGGAAGGAAA-3' and 5'-CCTGGTTTTGCATAGATG-3'; MOP9, TCGGGAAATGAAAATCC-3' and 5'-CCCAAAGCAAGTTAAAGC-3'. The InDel on F4F15 was amplified using the primers 5'-GAGCC-TATAATGAGCGTCG-3' and 5'-AAATGTCTCACGCGATGCG-3'.

DNA sequencing

To simplify sequencing of the *Arabidopsis cluA* homologue, we designed eight oligonucleotide primers to amplify the 8.064 kbp gene in four overlapping PCR fragments of 2–2.5 kbp. The four PCR fragments, generated using the proofreading DNA polymerase RedAccuTaq LA (Sigma Chemical Co., Poole, UK), were separated by agarose-gel electrophoresis and purified using the Qiagen minElute kit (Qiagen, Crawley, UK). DNA sequencing was performed using a BigDye Terminator v.3.1 Cycle Sequencing Kit and an ABI Prism 377 DNA sequencer (Applied Biosystems, Foster City, USA).

SAIL T-DNA insertion mutants

The Syngenta *Arabidopsis* Insertion Library (http://tmri.org/pages/collaborations/garlic_files/) was searched using the sequence of At3g52140 from start to stop codon, including introns (Accession: NC_003074). Three lines were identified with T-DNA left-border flanking sequences giving low *e*-values (SAIL_284_D06, e^0 ; SAIL_559_F01, e^{-149} ; SAIL_267b_D05, $9e^{-59}$). Seed of these lines was obtained from Syngenta Biotechnology Inc. (Research Triangle Park, NC, USA) and bulked up in the glasshouse without selection.

Plant transformation

Seed of each SAIL line was sown onto a 2 : 1 mixture of compost and vermiculite. When the plants were 2 weeks old, they were sprayed with glufosinate ammonia (BASTA) at $120 \mu\text{g l}^{-1}$ to select for plants containing the T-DNA insertion. These plants were stable-transformed with mitochondrial-targeted GFP by *Agrobacterium*-mediated transformation using the floral dip method (Clough and Bent, 1998). The infiltration medium contained $0.5\times$ MS salts, 5% (w/v) sucrose, 0.05% (w/v) Mes pH 5.7, $0.044 \mu\text{M}$ benzylaminopurine and 0.02% (v/v) Silwet L-77 (Lehle Seeds, Round Rock, USA). Briefly, the mitochondrial-GFP binary vector pBINmgfp5-atpase (Logan and Leaver, 2000) contains the N-terminal mitochondrial targeting sequence from the *N. plumbaginifolia* β -ATPase subunit upstream of mGFP5 (Siemering *et al.*, 1996) under the control of the CaMV 35S promoter (Logan and Leaver, 2000). Primary transformants were selected on MS-agar plates containing $50 \mu\text{g ml}^{-1}$ kanamycin and, after transfer to soil, by spraying with BASTA as above. Final selection was performed by epifluorescent microscopy to identify good GFP-expressing lines.

PCR analysis of putative homozygous insertion mutants

Syngenta *Arabidopsis* Insertion Library lines contain T-DNA insertions at known sites and the SAIL table available at http://www.tmri.org/pages/collaborations/garlic_files/plant_cell/ch3_main.htm gives details of gene-specific forward and reverse PCR primers that flank the predicted insertions on chromosome III. PCR primers flanking the insertion in line SAIL_284_D06 (5'-GGCTGCAAGGTTA-GGTATAAG-3' and 5'-TCGCCCCAGGGTGGTGT-3') were used in combination with a primer to the T-DNA left border (primer LB3-5'-TTCATAACCAATCTCGATACAC-3', Sessions *et al.*, 2002) to confirm the nature of the T-DNA insertion.

RNA isolation and gel-blot analysis

Total RNA was extracted from 7-day-old seedlings using a mini-RNA kit (Qiagen, Crawley, UK). Ten micrograms of RNA was fractionated in a denaturing 0.9% (w/v) agarose/formaldehyde gel and transferred to nitrocellulose according to standard procedures. Hybridisation was carried out in a formamide-containing buffer and followed by washing at high stringency ($0.2\times$ SSC, 0.1% (w/v) SDS, 42°C). Probes were labelled by random priming. The tubulin probe was prepared using a 1 : 1 : 1 mixture of four *Arabidopsis* beta-tubulin cDNAs (tub1–4) as template.

Acknowledgements

This research was supported by the Biotechnology and Biological Sciences Research Council under grant nos. 49G13350 and 49G1554 and by a research studentship to I.S. We thank Mr John Mackie for technical assistance with the electron microscopy and Mr Harry Hodge for technical assistance in the laboratory, glasshouse and growth rooms. The plasmids containing the *Arabidopsis* beta-tubulin cDNAs were cloned by Dr Sarah Scrase-Field, University of Southampton.

References

- Arimura, S. and Tsutsumi, N. (2002) A dynamin-like protein (ADL2b), rather than FtsZ, is involved in *Arabidopsis* mitochondrial division. *Proc. Natl. Acad. Sci. USA*, **99**, 5727–5731.

- Bell, C.J. and Ecker, J.R.** (1994) Assignment of 30 microsatellite loci to the linkage map of *Arabidopsis*. *Genomics*, **19**, 137–144.
- Bereiter-Hahn, J. and Voth, M.** (1994) Dynamics of mitochondria in living cells: shape changes, dislocations, fusion and fission of mitochondria. *Microscopy Res. Technique*, **27**, 198–219.
- Berger, K.H., Sogo, L.F. and Yaffe, M.P.** (1997) Mdm12p, a component required for mitochondrial inheritance that is conserved between budding and fission yeast. *J. Cell Biol.* **136**, 545–553.
- van der Bliek, A.M., Redelmeier, T.E., Dmake, E.J., Tisdale, E.M., Meyerowitz, E.M. and Schmid, S.L.** (1993) Mutations in human dynamin block an intermediate stage in coated vesicle formation. *J. Cell Biol.* **122**, 553–563.
- Browning, K.S., Gallie, D.R., Hershey, J.W., Heenebusch, A.G., Maitra, U., Merrick, W.C. and Norbury, C.** (2001) Unified nomenclature for the subunits of eukaryotic initiation factor 3. *Trends Biochem. Sci.* **26**, 284.
- Burgess, S.M., Delannoy, M. and Jensen, R.E.** (1994) MMM1 encodes a mitochondrial outer membrane protein essential for establishing and maintaining the structure of yeast mitochondria. *J. Cell Biol.* **126**, 1375–1391.
- Catlett, N.L. and Weisman, L.S.** (2000) Divide and multiply: organelle partitioning in yeast. *Curr. Opin. Cell Biol.* **12**, 509–516.
- Cervený, K.L., McCaffery, J.M. and Jensen, R.E.** (2001) Division of mitochondria requires a novel DNM1-interacting protein, Net2p. *Mol. Biol. Cell.* **12**, 309–321.
- Clough, S.J. and Bent, A.F.** (1998) Floral dip: a simplified method for *Agrobacterium*-mediated transformation of *Arabidopsis thaliana*. *Plant J.* **16**, 735–743.
- Damke, H.T., Baba, T., van der Bliek, A.M. and Schmid, S.L.** (1995) Clathrin-independent pinocytosis is induced in cells overexpressing a temperature-sensitive mutant of dynamin. *J. Cell Biol.* **131**, 69–80.
- Damke, H.T., Baba, T., Warnock, D.E. and Schmid, S.L.** (1994) Induction of mutant dynamin specifically blocks endocytic vesicle formation. *J. Cell Biol.* **127**, 915–934.
- Fekkes, P., Shepard, K.A. and Yaffe, M.P.** (2000) Gag3p, an outer membrane protein required for fission of mitochondrial tubules. *J. Cell Biol.* **151**, 333–340.
- Fields, S.D., Conrad, M.N. and Clarke, M.** (1998) The *S. cerevisiae* *CLU1* and *D. discoideum* *cluA* genes are functional homologues that influence mitochondrial morphology and distribution. *J. Cell Sci.* **111**, 1717–1727.
- Fields, S.D., Arana, Q., Heuser, J. and Clarke, M.** (2003) Mitochondrial membrane dynamics are altered in *cluA* mutants of *Dictyostelium*. *J. Muscle Res. Cell Motil.* (in press).
- Hales, K.G. and Fuller, M.T.** (1997) Developmentally regulated mitochondrial fusion by a conserved, novel, predicted GTPase. *Cell*, **90**, 121–129.
- Hermann, G.J., King, E.J. and Shaw, J.M.** (1997) The yeast gene MDM20, is necessary for mitochondrial inheritance and organization of the actin cytoskeleton. *J. Cell Biol.* **137**, 141–153.
- Herskovits, J.S., Burgess, C.C., Obar, R.A. and Vallee, R.B.** (1993) Effects of mutant rat dynamin on endocytosis. *J. Cell Biol.* **122**, 565–578.
- Hinshaw, J.E. and Schmid, S.L.** (1995) Dynamin self-assembles into rings suggesting a mechanism for coated vesicle budding. *Nature*, **374**, 190–192.
- Jander, G., Norris, S.R., Rounsley, S.D., Bush, D.F., Levin, I. and Last, R.L.** (2002) *Arabidopsis* map-based cloning in the post-genome era. *Plant Physiol.* **129**, 440–450.
- Kennedy, E.P. and Lehninger, A.L.** (1949) Oxidation of fatty acids and tricarboxylic acid cycle intermediates by isolated rat liver mitochondria. *J. Biol. Chem.* **179**, 957–972.
- Khodjakov, A., Lizunova, E.M., Minin, A.A., Koonce, M.P. and Gyoeva, F.K.** (1998) A specific light chain of kinesin associates with mitochondria in cultured cells. *Mol. Biol. Cell*, **9**, 333–343.
- Konieczny, A. and Ausubel, F.M.** (1993) A procedure for mapping *Arabidopsis* mutations using co-dominant ecotype-specific PCR-based markers. *Plant J.* **4**, 403–410.
- Labrousse, A.M., Zappaterra, M.D., Rube, D.A. and van der Bliek, A.M.** (1999) *C. elegans* dynamin-related protein DRP-1 controls severing of the mitochondrial outer membrane. *Mol. Cell*, **4**, 815–826.
- Logan, D.C. and Leaver, C.J.** (2000) Mitochondria-targeted GFP highlights the heterogeneity of mitochondrial shape, size and movement within living plant cells. *J. Exp. Bot.* **51**, 865–871.
- Lukowitz, W., Gillmor, C.S. and Scheible, W.-R.** (2000) Positional cloning in *Arabidopsis*. Why it feels good to have a genome initiative working for you. *Plant Physiol.* **123**, 795–805.
- Marrison, J.L., Rutherford, S.M., Robertson, E.J., Lister, C., Dean, C. and Leech, R.M.** (1999) The distinctive roles of five different ARC genes in the chloroplast division process in *Arabidopsis*. *Plant J.* **18**, 651–662.
- McConnell, S.J. and Yaffe, M.P.** (1992) Nuclear and mitochondrial inheritance in yeast depends on novel cytoplasmic structures defined by the MDM1 protein. *J. Cell Biol.* **118**, 385–395.
- Mozy, A.D., McCaffery, J.M. and Shaw, J.M.** (2000) Dnm1p GTPase-mediated mitochondrial fission is a multi-step process requiring the novel integral membrane component Fis1p. *J. Cell Biol.* **151**, 367–379.
- Nishida, K., Takahara, M., Miyagishima, S.Y., Kuroiwa, H., Matsuzaki, M. and Kuroiwa, T.** (2003) Dynamic recruitment of dynamin for final mitochondrial severance in a primitive red alga. *Proc. Natl. Acad. Sci. USA*, **100**, 2146–2151.
- Olyslaegers, G. and Verbelen, J.-P.** (1998) Improved staining of F-actin and co-localization of mitochondria in plant cells. *J. Microsc.* **192**, 73–77.
- Ostuga, D., Keegan, B.R., Brisch, E., Thatcher, J.W., Hermann, G.J., Bleazard, W. and Shaw, J.** (1998) The dynamin-related GTPase, Dnm1p, controls mitochondrial morphology in yeast. *J. Cell Biol.* **143**, 333–349.
- Pye, K.A. and Leech, R.M.** (1992) Chloroplast division and expansion is radically altered by nuclear mutations in *Arabidopsis thaliana*. *Plant Physiol.* **99**, 1005–1008.
- Pye, K.A. and Leech, R.M.** (1994) A genetic-analysis of chloroplast division and expansion in *Arabidopsis thaliana*. *Plant Physiol.* **104**, 201–207.
- Pye, K.A., Rutherford, S.M., Robertson, E.J. and Leech, R.M.** (1994) *arc6*, a fertile *Arabidopsis* mutant with only 2 mesophyll cell chloroplasts. *Plant Physiol.* **106**, 1169–1177.
- Sessions, A., Burke, E., Presting, G. et al.** (2002) A high-throughput *Arabidopsis* reverse genetics system. *Plant Cell*, **14**, 2985–2994.
- Shaw, J.M. and Nunnari, J.** (2002) Mitochondrial dynamics and division in budding yeast. *Trends Cell Biol.* **12**, 178–184.
- Shepard, K.A. and Yaffe, M.P.** (1997) Genetic and molecular analysis of Mdm14p and Mdm17p, proteins involved in organelle inheritance. *Mol. Biol. Cell*, **8** (Suppl.), 2585–2585.
- Siemering, K.R., Golbik, R., Sever, R. and Haseloff, J.** (1996) Mutations that suppress the thermosensitivity of green fluorescent protein. *Curr. Biol.* **6**, 1653–1663.
- Smirnova, E., Shurland, D.-L., Ryazanov, S.N. and van der Bliek, A.M.** (1998) A human dynamin-related protein controls the distribution of mitochondria. *J. Cell Biol.* **143**, 351–358.

- Stenoien, D.L. and Brady, S.T.** (1997) Immunochemical analysis of kinesin light chain function. *Mol. Biol. Cell*, **8**, 675–689.
- Stevens, B.J.** (1977) Variation in number and volume of the mitochondria in yeast according to growth conditions. A study based on serial sectioning and computer graphics reconstruction. *Biol. Cell*, **28**, 37–56.
- Stickens, D. and Verbelen, J.P.** (1996) Spatial structure of mitochondria and ER denotes changes in cell physiology of cultured tobacco protoplasts. *Plant J.* **9**, 85–92.
- Tieu, Q. and Nunnari, J.** (2000) Mdv1p is a WD repeat protein that interacts with the dynamin-related GTPase Dnm1p, to trigger mitochondrial division. *J. Cell Biol.* **151**, 353–365.
- Van Gestel, K., Kohler, R.H. and Verbelen, J.-P.** (2002) Plant mitochondria move on F-actin, but their positioning in the cortical cytoplasm depends on both F-actin and microtubules. *J. Exp. Bot.* **53**, 659–667.
- Verhey, K.J., Meyer, D., Deehan, R., Blenis, J., Schnapp, B.J., Rapoport, T.A. and Margolis, B.** (2001) Cargo of kinesin identified as JIP scaffolding proteins and associated signalling molecules. *J. Cell Biol.* **152**, 959–970.
- Vornlocher, H.P., Hanachi, P., Ribeiro, S. and Hershey, J.W.** (1999) A 110-kilodalton subunit of translation initiation factor eIF3 and an associated 135-kilodalton protein are encoded by the *Saccharomyces cerevisiae* TIF32 and TIF31 genes. *J. Biol. Chem.* **274**, 16802–16812.
- Yaffe, M.P.** (1999) The machinery of mitochondrial inheritance and behavior. *Science*, **283**, 1493–1497.
- Zhu, Q., Hulén, D., Liu, T. and Clarke, M.** (1997) The *cluA*⁻ mutant of *Dictyostelium* identifies a novel class of proteins required for dispersion of mitochondria. *Proc. Natl. Acad. Sci. USA*, **94**, 7308–7311.